Available online at www.sciencedirect.com
SCIENCE DIRECT®
International Journal of Heat and Mass Transfer 48 (2005) 4615–4622
International Journal of HEAT and MASS TRANSFER
www.elsevier.com/locate/ijhmt

CHF characteristics and correlations of concentric-tube open thermosyphon working with R22

M. Ashraful Islam [a,*], Masanori Monde [b,1], Yuichi Mitsutake [b,2]

[a] Department of Mechanical Engineering, BUET, Dhaka 1000, Bangladesh
[b] Department of Mechanical Engineering, Saga University, 1 Honjo, Saga 840-8502, Japan

Received 5 January 2005
Available online 25 July 2005

Abstract

Experiments are performed to understand the critical heat flux (CHF) mechanism in a concentric-tube open thermosyphon working with R22. An electrically heated bottom-closed outer tube with an unheated inner tube inserted concentrically serves as an evaporator of the thermosyphon. CHF data are collected by using saturated R22 at 1.5, 2.0 and 2.5 MPa by varying different geometrical parameters of the thermosyphon. For a particular outer tube, there is an optimum diameter of the inner tube for which the CHF is maximum. The optimum diameter of the inner tube is about half of the diameter of the outer tube and divides the CHF into two characteristic regions. Available correlations for predicting the CHF in each region are compared with the present data and more generalized correlations have been proposed.

Keywords: Thermosyphon; Critical heat flux; Concentric tube; CHF enhancement

1. Introduction

A thermosyphon is a device, which transfers heat, mass and momentum by utilizing buoyancy force acting on a fluid contained in a vessel. Heat transfer characteristics and the critical heat flux (CHF) in thermosyphon have been studied for many years to apply it for cooling electronic circuits and gas turbine blades, extracting geothermal energy, preserving permafrost, etc. The effective thermal conductivity in thermosyphon can be significantly improved by inserting a tube concentrically into it. This is attributed to the fact that the inner tube enables liquid to be supplied to the thermosyphon without any interaction with the escaping vapor flow. It seems that there are considerable studies on concentric-tube thermosyphon and some of these include the studies of Seki et al. [1,2] and Mitsutake et al. [3]. Most recently in 1998 Islam et al. [4,5] carried out experimental studies on concentric-tube thermosyphon to collect the CHF data for water, ethanol and R113, and discussed the fundamentals of CHF mechanism and proposed correlations for predicting the CHF.

* Corresponding author. Present address: C/O Professor M. Monde, Department of Mechanical Engineering, Saga University, 1 Honjo, Saga 840-8502, Japan. Tel.: +880 2 9665636; fax: +880 2 8613046.
E-mail addresses: aislam@me.buet.ac.bd (M.A. Islam), monde@me.saga-u.ac.jp (M. Monde), mitutake@me.saga-u.ac.jp (Y. Mitsutake).
[1] Tel.: +81 952 28 8608; fax: +81 952 28 8587.
[2] Tel.: +81 952 28 8616; fax: +81 952 28 8587.

0017-9310/$ - see front matter © 2005 Elsevier Ltd. All rights reserved.
doi:10.1016/j.ijheatmasstransfer.2005.03.033

Nomenclature

C	constant
D_{he}	equivalent heated diameter, $(D_i^2 - d_o^2)/D_i =$ (4 × cross-sectional area/heater perimeter)
D_i	inner diameter of the outer heated tube [mm]
d_i	inner diameter of the inner unheated tube [mm]
d_o	outer diameter of the inner unheated tube [mm]
g	gravitational acceleration [m s^{-2}]
H_{fg}	latent heat of vaporization [kJ kg^{-1}]
Ku	Kutateladze number $= [q_{co}/(\rho_v H_{fg})]/\sqrt[4]{\sigma g(\rho_l - \rho_v)/\rho_v^2}$
L	heated tube length [mm]
P	system pressure [MPa]
q_{co}	CHF for saturated boiling [MW m^{-2}]
$q_{co,0}$	q_{co} without inner tube [MW m^{-2}]
s	annular gap, $(D_i - d_o)/2$ [mm]
t	wall thickness of the inner tube [mm]

Greek symbols

Φ	$=(4L/D_i)Ku$
Φ_r	$=(4L/D_{he})Ku$
Φ^*	$=\Phi/[0.16(\rho_l/\rho_v)^{0.13}]$
Φ_r^*	$=\Phi_r/[0.64(\rho_l/\rho_v)^{0.13}]$
ρ	density [kg m^{-3}]
σ	surface tension [N m^{-1}]

Subscripts

he	heated equivalent
fg	liquid–vapor phase-change
i	inner
l	liquid
o	outer
r	revised
v	vapor

Islam et al. [4] found that for a fixed diameter outer tube, there exists an optimum diameter of the inner tube for which the CHF is maximum. The optimum diameter of the inner tube, $d_{o,opt}$ divides the CHF into two characteristics regions, Region I and Region II. The CHF of Region I can be predicted by Eq. (1) within ±30%.

$$\Phi^* = 4\left[1 + C\frac{d_i}{D_i + d_o}\right] \tag{1}$$

where $C = 0.803[L/\sqrt{\sigma/g(\rho_l - \rho_v)}]^{0.5}$.

Again, the CHF of Region II is comparable to natural convective boiling (NCB) in vertical circular annuli and can be predicted by Eq. (2) within ±30%.

$$Ku = \frac{0.16}{1 + 0.075(L/D_{he})} \tag{2}$$

which is proposed by Monde et al. [6] in 1994 for predicting the CHF during NCB in vertical annuli where inner tube is heated. It can be mentioned that heating of either inner tube or outer tube of the annulus has negligible effect on the CHF belonging to Region II.

The study by Islam et al. [5] on the concentric-tube thermosyphon is for $L/D_i = 6$–200, $s = 1$–6 mm and for the density ratio $\rho_l/\rho_v = 67.6$–1605.2 with Ethanol, R113 and Water as working fluids. The present study is devoted to the concentric-tube thermosyphon with the same geometrical parameters working with R22 having the density ratio $\rho_l/\rho_v = 8.8$–17.5 in order to have the CHF data in a wide range of the density ratio. It is understood that R22 is a CFC fluid detrimental to the global environment. For the sake of academic interest, experiments are conducted using R22 as a working fluid. The present experimental conditions are given in Table 1.

Table 1
Experimental conditions

Working fluid	R22
P [MPa]	1.5, 2.0, and 2.5
ρ_l/ρ_v [–]	8.76, 12.04, and 17.45
L [mm]	1000, 500, 250, and 100
$D_i(d_o)$ [mm(mm)]	17(15,13,11,9,7,5,0) 12(10,8,7,6,5,4,0) 9(7,6,5,4,3,0), 5(0,3)
s [mm]	1–6
t [mm]	0.5–1

In this study, the CHF characteristics and the effects of different parameters on the CHF of R22 in concentric-tube thermosyphon are presented as done before for water, R113 and ethanol [5]. The CHF data in respective regions of the thermosyphons are compared with the existing correlations (1) and (2), and a more generalized correlation for Region I has been proposed. Prediction of maximum CHF is also prescribed here.

2. Experiment

2.1. Test facility

The test facility to measure the CHF in the present thermosyphon is shown in Fig. 1. It consists of a pressure vessel, a heating system, and a data acquisition.

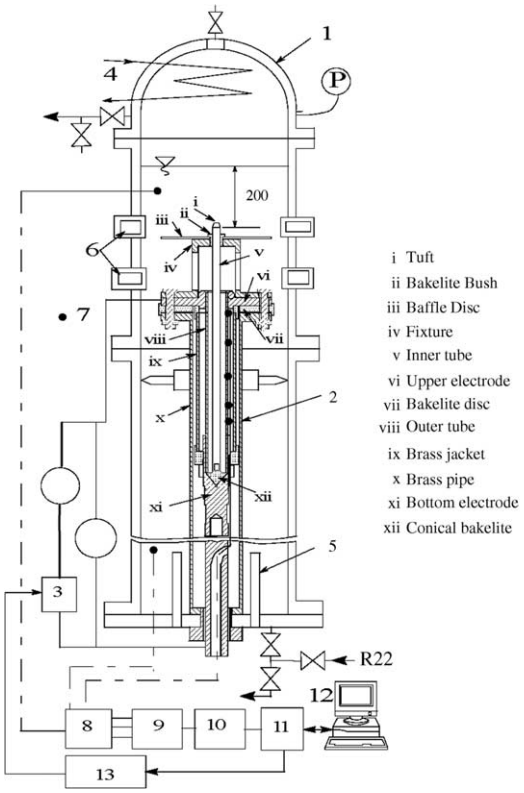

Fig. 1. A schematic of the experimental apparatus where the numbered items are: 1—pressure vessel, 2—thermosyphon assembly, 3—DC power supply, 4—cooling coil, 5—auxiliary heater, 6—windows, 7—thermocouple locations, 8—ice box, 9—multiplexer, 10—digital thermometer, 11—GPIB, 12—computer, 13—GPIB programmer.

The pressure vessel contains the thermosyphon assembly and test fluid. Auxiliary heaters and cooling coils are also placed in the vessel to maintain the system pressure at a designated saturation temperature. Several windows are provided on the vessel for flow observation at the exit of the thermosyphon.

The detailed description of the thermosyphon assembly and the heating system and data acquisition system is given in the previous studies [4,5].

2.2. Procedure

The pressure vessel is first filled with the test liquid up to 200 mm above the top of the inner tube. This extra liquid head is provided in order to stabilize the system pressure. The liquid is heated up to the saturation temperature at the designated pressure by auxiliary heaters. The saturated condition is maintained by thermostatically adjusting the power input to the heaters and by regulating the water flow rate in the cooling circuit. At the steady state condition, the heat is added to the thermosyphon tube in steps from the DC power supply. After each voltage increase, instantaneous local wall temperatures of the heated tube are monitored and compared with the temperature of the fluid bath. The wall temperature, at a certain heat flux and location, starts running away or increasing monotonically and then the CHF is defined to have occurred. As soon as the CHF is detected, the power supply is automatically cut off when the difference between the wall and saturation temperatures is beyond 80 K. Near the CHF, the voltage increment is not more than 1% of the preceding voltage step, which ensures the total uncertainty in the CHF data to be within 3%. Three consecutive runs are conducted for each experimental condition and the data reproducibility is confirmed within 3%.

3. Results and discussion

The critical heat flux (CHF) in the present concentric-tube thermosyphons has been defined as the heat flux which leads to the wall temperature excursion of the heated tube and a great many CHF data are collected by varying different parameters listed in Table 1. About 700 experimental runs were made to collect about 600 CHF data for R22. Instantaneous wall temperatures at the outer tube of the thermosyphon for different experimental conditions have also been recorded in order to get boiling curves and the CHF location as well. For all the concentric-tube thermosyphon, the CHF occurred near the top of the outer tube, while for conventional thermosyphon it occurred near the bottom of the outer tube. The CHF location has been explained clearly elsewhere when water was the working fluid [4]. The flow condition at the open end of the thermosyphon is observed to have some information concerning the CHF mechanism.

3.1. CHF in conventional thermosyphons

In the present experiment, a great many CHF data have been collected without being inserted an inner tube in the thermosyphon in order to evaluate the effects of inner tube and compare these with the existing CHF data for conventional thermosyphons. Accordingly, Fig. 2 has been constructed with a view to explaining the basic CHF characteristics of R22.

Fig. 2 represents all the CHF data without the inner tube plotted against the density ratio (ρ_l/ρ_v). The data for R113 are also plotted here for comparison. The solid line is the Kutateladze correlation for predicting the CHF in an ordinary saturated pool boiling. Each of the symbols represents CHF data for a particular combination of length and diameter of the outer tube.

Fig. 2 shows that the CHF basically depends on the ratio L/D_i and ρ_l/ρ_v and that its character for the same

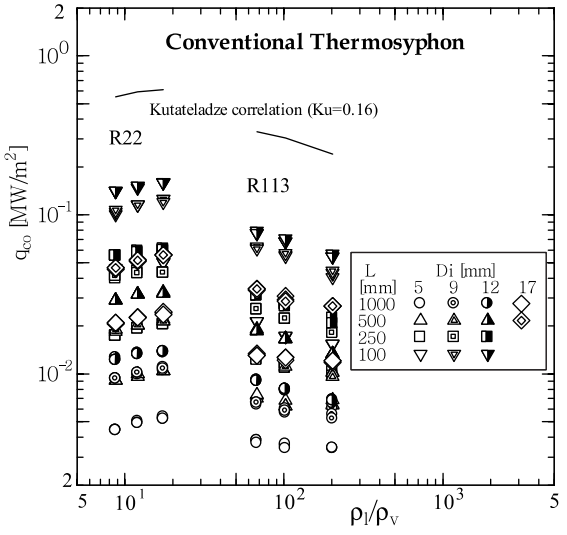

Fig. 2. Characteristics of the CHF.

value of L/D_i has a tendency similar to the Kutateladze's prediction for saturated pool boiling, but its value is smaller because boiling occurs in the narrow confines of the tube in the case of thermosyphon. For the same value of L/D_i, the CHF increases with an increase in ρ_l/ρ_v for R22, while decreases for R113. This is because of the working pressures chosen in this study such that the reduced pressure, P_r, is in the range of 0.301–0.501 for R22 while P_r was much less than 0.3 for R113. It is well known that the CHF increases with P_r and becomes maximum at a working pressure having $P_r = 1/3$ beyond which it decreases continuously [7]. As P_r inversely varies with ρ_l/ρ_v, the CHF as shown in Fig. 2 is obtained.

Eq. (3) proposed by Imura et al. [8] in 1983 is one of the widely accepted correlations for closed two-phase conventional thermosyphons while Eq. (4) is proposed by Tien and Chung [9] based on the flooding criterion for predicting the CHF in similar type of thermosyphons. In 1996, Monde [10] developed an analytical model to evaluate the CHF in a two-phase thermosyphon from the maximum falling liquid flow rate into the thermosyphon tube during a countercurrent vapor–liquid flow in it.

$$\Phi = 0.64(\rho_l/\rho_v)^{0.13} \tag{3}$$

$$\Phi = 3.2\tanh(0.5Bo^{1/4})/[1+(\rho_v/\rho_l)^{1/4}]^2 \tag{4}$$

with $Bo = D_i/[\sigma/g(\rho_l-\rho_v)]^{1/2}$.

Fig. 3 shows the parameter Φ, the non-dimensional parameter commonly used for the CHF in conventional thermosyphon (which is also equal to Φ_r for $d_o = 0$), as a function of the density ratio, ρ_l/ρ_v. Along with R22, the CHF data for water and R113 of previous studies [4,5] are also plotted here for complete understanding of

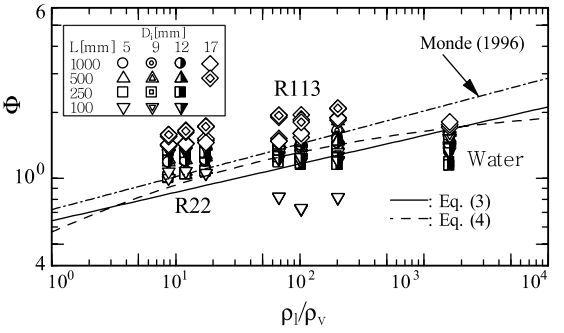

Fig. 3. Comparison of conventional CHF data with existing predictions.

CHF characteristics. Different lines are the predictions by Monde [10], correlations (3) and (4), and are shown here for comparison. The correlation (4) of Tien and Chung [9] is plotted tentatively for $Bo = 10$, because Bo falls in the range of 2.0–27.8 for the present experimental range and the effect of Bo on CHF is negligibly small [10]. Fig. 3 shows that the CHF data are in a moderate agreement with correlations (3) and (4), and the Monde prediction. All the existing works under-predict some data for R113 and R22, while over-predict some data for water. However, the correlation (3) proposed by Imura et al. [8] has been chosen as a reference to correlate the CHF data of Region I for concentric-tube open thermosyphon as done before [4,5].

3.2. Effects of inner tube on CHF

The collection of CHF data in the concentric-tube thermosyphons having fixed length and diameter of the outer tube with different inner tubes is the primary objective of a series of experiments in the present study. These data tell us the most suitable combination of inner and outer tubes for maximizing the heat transfer limit.

Fig. 4 shows a typical variation of the CHF with the inner tube diameter of the thermosyphons having a fixed

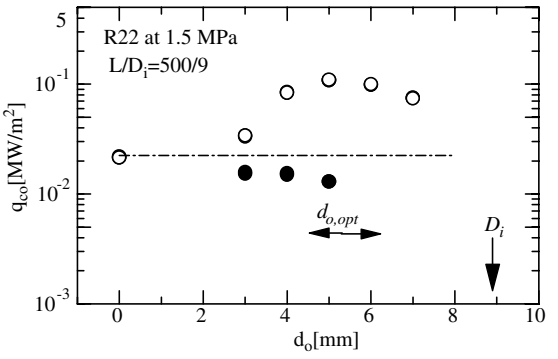

Fig. 4. Effects of inner tube on CHF.

outer tube of $L/D_i = 500/9$ working with R22 at 1.5 MPa. The solid circular symbol represents the CHF data with a rod inserted concentrically into the outer tube. The horizontal line is the mark of the value of CHF of conventional thermosyphon and it clearly demonstrates the effect of liquid supply through the inner tube in a concentric-tube thermosyphon on CHF improvement. Inner tube helps supply liquid to ensure continuity as vapor forms in the annulus and enhances the CHF as shown, while solid rod imposes more restriction to liquid supply to the annulus and makes a decrease in the CHF value. For $d_o = 3$ mm, the CHF enhancement is retarded a little compared to the next larger inner tube, which was also observed for other working fluids for longer thermosyphon. The reason of this anomaly may in part be due to capillary effect as the diameter of the inner tube becomes too small to allow liquid to flow through it.

From Fig. 4, one can notice that the CHF enhancement increases up to a certain diameter of the inner tube and then decreases as the inner tube diameter approaches the outer tube diameter. There exists, as depicted in the figure, an optimum outer diameter of the inner tube that maximizes the CHF and its value is about half of the outer tube diameter. The horizontal line with solid arrow heads gives the possible range of the optimum inner tube diameter, $d_{o,opt}$.

Other than d_o, the CHF in a concentric-tube thermosyphon is influenced by the length L of the outer tube, by the diameter D_i of the outer tube, by the working pressure P, and by the working fluid as well. The effects of these parameters are shown in Fig. 5(a)–(c) and are described briefly.

Fig. 5(a) depicts the variation of the CHF with the inner tube diameter d_o for $D_i = 12$ mm working with R22 at 1.5 MPa, where different symbols are for different lengths of the outer tube. The CHF increases with decreasing tube length for any inner tube diameter. It is clear from this figure that the length L seems to have negligible effect on the optimum diameter of the inner tube, $d_{o,opt}$.

Fig. 5(b) exhibits the CHF variation with the inner tube diameter d_o for $L = 1000$ mm at a working pressure of 1.5 MPa, where different symbols are for different diameter of the outer tube. It is clear from Fig. 5(b) that the diameter D_i of the outer tube strongly influences the optimum diameter of the inner tube, $d_{o,opt}$. The approximate values of $d_{o,opt}$ for $D_i = 17$, 12 and 9 mm are, respectively, 9, 7, and 5 mm; these are about half of the inner diameter of the outer tube.

Fig. 5(c) shows the CHF variation with inner tube diameter d_o for a fixed outer tube of $L/D_i = 1000/12$ at three different system pressures. Different lines in the figure show Eq. (3) of Imura et al. [8] for different pressures. As shown in the figure, the effect of the system pressure on the CHF is slightly prominent near the optimum diameter of the inner tube, while this effect is reduced as d_o approaches to both limiting cases, namely $d_o \to 0$ or D_i and the reasons of such tendency variation are not clear yet. Fig. 5(c) also demonstrates that system pressure has negligible effect on the optimum diameter of the inner tube.

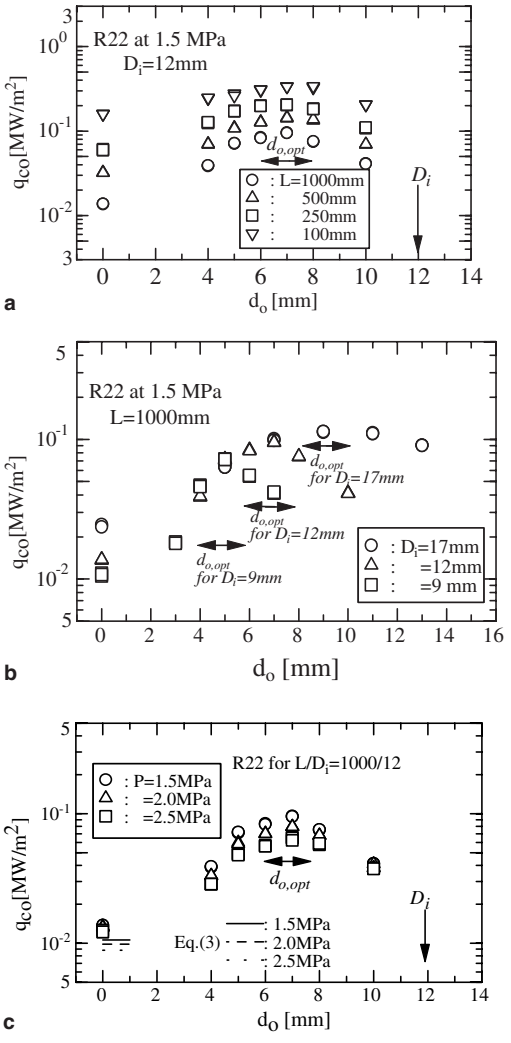

Fig. 5. Effect of (a) L, (b) D_i and (c) P on CHF.

4. CHF correlations

The CHF data in the concentric-tube thermosyphons have been categorized into two characteristic regions, Regions I and II, with respect to the optimum diameter, $d_{o,opt}$ as reported in the previous studies [4,5] where the characteristics of CHF in both the regions are clearly described and correlations are proposed for predicting the CHF in the respective regions. The CHF data of R22

belonging to each region are compared and analyzed more critically in this section.

4.1. Region I ($d_o < D_i/2$)

In this region, enhancement in the CHF value is perhaps achieved by some amount of liquid supplied through the inner tube while some liquid still enters the annulus obstructing vapor flow as observed during experiments. At the optimum diameter of the inner tube, the liquid flow in the concentric-tube thermosyphon becomes co-current having no obstructing liquid anymore through the annulus and the CHF becomes maximum.

All the CHF data of Region I for R22 are plotted on the coordinates of Φ^* versus $Cd_i/(D_i + d_o)$ in Fig. 6 where the solid line is Eq. (1) that can predict only 60% of the CHF data within ±30% error while it predicted well all the CHF for Water, Ethanol and R113 within this limit reported previously [4]. Fig. 6 tells about the need for revising the correlation to formulate a generalized one that can predict CHF data for all the working fluids.

Eq. (1) has been so chosen that it becomes correlation (3) when there is no inner tube. The CHF dependence on inner tube is taken into account only the ratio of frictional area, $d_i/(D_i + d_o)$ and it might be incorrect as this fails to predict all the data. Now it has been realized that the ratio of heated surface and flow area of annulus plays an important role in this region in addition to the ratio of frictional flow area. Thus, the $\Phi = (4L/D_i)Ku$ has been revised as $\Phi_r = (4L/D_{he})Ku$ using equivalent heated diameter, D_{he}, in place of outer tube diameter, D_i and consequently Φ_r^* is chosen as the non-dimensional dependent variable to correlate CHF data in this region as given by Eq. (5).

$$\Phi_r^* = 1 + C\frac{d_i}{D_i + d_o} \tag{5}$$

Eq. (5) becomes correlation (3) when there is no inner tube; that is, conventional thermosyphon. The value of

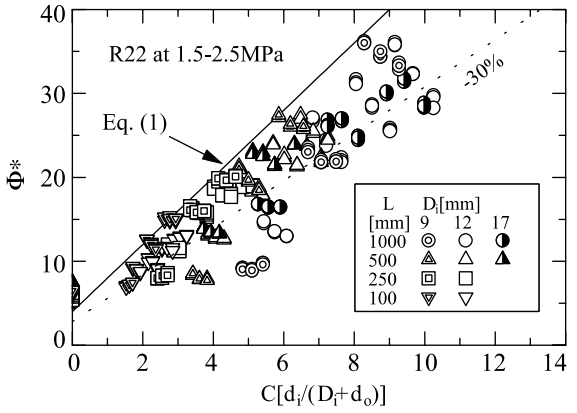

Fig. 6. Comparison of CHF data of Region I.

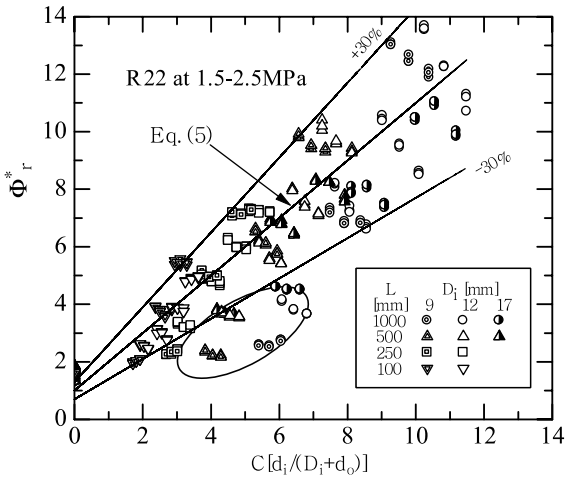

Fig. 7. Revised correlation for CHF data of Region I for R22.

C is strongly influenced by the length of the thermosyphon and the working fluids as also mentioned in the previous study [4]. It is also revised by analyzing graphs of Φ_r^* versus $d_i/(D_i + d_o)$ for R22 and can be approximated by Eq. (6) with ±20%.

$$C = 0.9[L/\sqrt{\sigma/g(\rho_l - \rho_v)}]^{0.5} \tag{6}$$

Fig. 7 correlates all the CHF data of R22 belonging to Region I. It is found that the CHF data can be predicted well by Eq. (5) within ±30% except for few cases (encircled in the figure) where diameter of the inner tube is smaller for longer thermosyphons. It may be mentioned here that the longer small-diameter inner tube works as capillary tube, imparts more restriction and experiences more fluid friction resulting in lower CHF values (cf. Fig. 4) compared to the next larger diameter inner tube. This was also common for other working fluids experimented with and published elsewhere previously [4,5]. The performance of the revised correlation (5) has been tested for predicting CHF in Region I working with other fluids. Fig. 8 exhibits such performance for R113, ethanol and water. It is clear from this figure that correlation (5) can well predict the CHF data belonging to Region I.

4.2. Region II ($d_o > D_i/2$)

The flow situation in concentric-tube thermosyphon having $d_o > d_{o,opt}$ (Region II) is almost similar to the natural convection boiling in vertical circular annuli as mentioned by Islam et al. [4,5] and the CHF can be predicted by existing correlation (2). Therefore, Fig. 9 has been constructed considering the variables of Eq. (2) and all the CHF data for R22 in this region are compared accordingly. From this figure, it is clear that the CHF data in this region can be predicted well by Eq. (2) with a standard deviation of 24%.

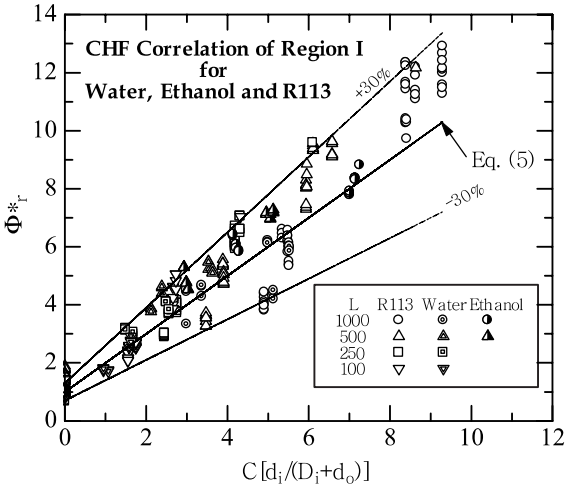

Fig. 8. Revised correlation for CHF data of Region I other than R22.

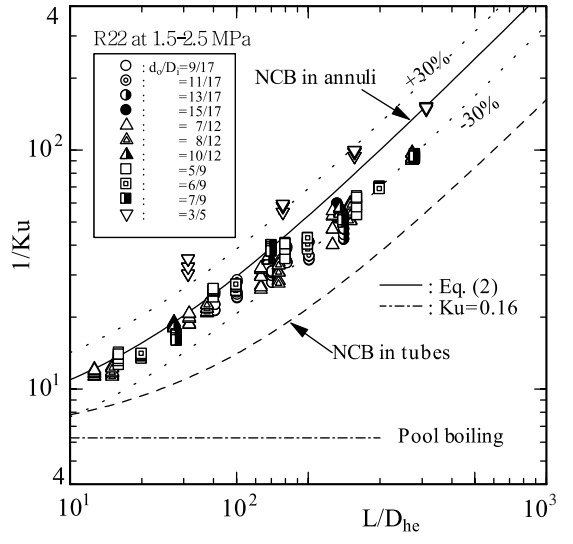

Fig. 9. Comparison of CHF data of Region II for R22.

4.3. Prediction of maximum CHF

It is understood from the previous studies [4,5] and from present analysis that for a particular length–diameter combination of the concentric-tube thermosyphon, there exists a maximum CHF when an inner tube of diameter is about half of that of the outer tube. This maximum CHF can either be calculated by using Eq. (2) or Eq. (5) for a specific geometry of the outer tube and working condition. The calculation of the maximum CHF for different experimental conditions has been made using both Eq. (2) and Eq. (5) for $d_o = D_i/2$. The calculated values are then compared with experimental values and analyzed accordingly.

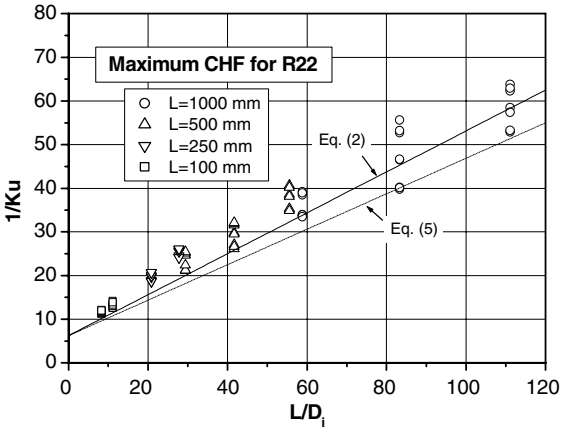

Fig. 10. Prediction of maximum CHF for R22.

The maximum CHF in concentric tube thermosyphon is the function of length/diameter of the outer tube and working fluid. Working pressure has some effect on the magnitude of maximum CHF as shown in Fig. 5(c). Tentatively reciprocal of Kutateladze number, *Ku* for R22 has been plotted against L/D_i in Fig. 10 where different lines are for maximum CHF calculated by Eq. (2) and Eq. (5). The experimental maximum CHF values are almost close to those predicted by Eq. (2), while Eq. (5) over-predicts more with the increase in L/D_i. It is worth mentioning that prediction of maximum CHF is very important from the engineering view point as engineers would look for it in designing a proper heat transfer device of this type. Further study is necessary for predicting the maximum CHF more precisely.

5. Conclusions

The CHF data in the concentric-tube open thermosyphons for R22 are presented. From the analysis of the data, the following conclusions are drawn:

1. The CHF in a concentric-tube thermosyphon is enhanced several times compared with that in a conventional one.
2. For a particular heated tube diameter working with a specific fluid, there is an optimum diameter of the inner tube at which the CHF is maximum and it is about half of the diameter of the outer tube. The length and working fluid of the thermosyphon have negligible effect on this.
3. The optimum diameter of the inner tube divides the CHF into two characteristic regions. The CHF in Region I appears to be comparable to that in a conventional thermosyphon and the CHF in Region II seems to be similar to that in a natural convective boiling in vertical circular annuli.

4. Most of the CHF data in Region I can be predicted well by Eq. (5) within ±30%.
5. Most of the CHF data in Region II can be predicted by Eq. (2) within ±30%.

Acknowledgement

Authors gratefully acknowledge the contribution of Saga University, Japan for providing facilities in conducting experiments.

References

[1] N. Seki, S. Fukusako, K. Koguchi, An experimental investigation of boiling heat transfer of fluorocarbon R-11 refrigerant for concentric-tube thermosyphon, Trans. ASME, J. Heat Transfer 103 (1981) 472–477.
[2] N. Seki, S. Fukusako, K. Koguchi, Single-phase heat transfer characteristics of concentric-tube thermosyphon, Wärme Stoffübertrag. 14 (1980) 189–199.
[3] Y. Mitsutake, M. Monde, M.Z. Hasan, Experimental study of the critical heat flux in open concentric-tube thermosyphon, in: Proceedings of the 3rd KSME–JSME Thermal Engineering Conference, Kyongyu, October, 1996, pp. 71–76.
[4] M.A. Islam, M. Monde, M.Z. Hasan, Y. Mitsutake, Experimental study of CHF in concentric-tube open thermosyphon, Int. J. Heat Mass Transfer 41 (1998) 3691–3704.
[5] M.A. Islam, M. Monde, M.Z. Hasan, Y. Mitsutake, An experimental investigation of CHF in an open concentric-tube thermosyphon, Heat Transfer 1998, in: Proceedings of the 11th International Heat Transfer Conference, Kyongju, Korea, vol. 2, 1998, pp. 181–186.
[6] M. Monde, Y. Mitsutake, S. Kubo, Critical heat flux during natural convective boiling in a vertical uniformly heated inner tubes in vertical annular tubes submerged in saturated liquid, Wärme Stoffübertrag. 29 (1994) 271–276.
[7] K. Stephan, Heat Transfer in Condensation and Boiling, Springer-Verlag, 1987, pp. 160–161.
[8] H. Imura, K. Sasaguchi, H. Kozai, S. Numata, Critical heat flux in a closed two-phase thermosyphon, Int. J. Heat Mass Transfer 26 (1983) 1181–1188.
[9] C.L. Tien, K.S. Chung, Entrainment limits in heat pipes, AIAA J. 17 (1979) 643–646.
[10] M. Monde, Analytical study of critical heat flux in two-phase thermosyphon: relationship between maximum falling liquid rate and critical heat flux, Trans. ASME, J. Heat Transfer 118 (1996) 422–428.